

sequestration potential under existing agroforestry systems for any district or region.

1. Bargali, S. S., Bargali, K., Singh, L., Ghosh, L. and Lakhera, M. L., *Acacia nilotica* based traditional agroforestry system: effect on paddy crop and management. *Curr. Sci.*, 2009, **96**(4), 581–587.
2. Parihaar, R. S., Bargali, K. and Bargali, S. S., Status of an indigeneous agroforestry system: a case study in Kumaun Himalaya. *Indian J. Agric. Sci.*, 2015, **85**(3), 442–447.
3. Unruh, J. D. and Lefebvre, P. A., A spatial database for estimating areas for agroforestry in Sub-Saharan Africa: aggregation and use of agroforestry case studies. *Agrofor. Syst.*, 1995, **32**, 81–96.
4. Pathak, P. S., Pateria, H. M. and Solanki, K. R., *Agroforestry Systems in India: A Diagnosis and Design Approach*, NRCFAF (ICAR), New Delhi, 2000.
5. FSI, *State of Forest Report*, Forest Survey of India (Ministry of Environment & Forests), Dehradun, 2013.
6. Dhyani, S. K., National Agroforestry Policy 2014 and need for area estimation under agroforestry. *Curr. Sci.*, 2014, **107**(1), 9–10.
7. Nair, P. K. R., Kumar, B. M. and Nair, V. D., Agroforestry as a strategy for carbon sequestration. *J. Plant Nutr. Soil Sci.*, 2009, **172**, 10–23.
8. Zomer, R. J., Trabucco, A., Coe, R. and Place, F., *Trees in Farm: Analysis of Global Extent and Geographical Patterns of Agroforestry*, ICRAF Working Paper no. 89, World Agroforestry Center, Nairobi, Kenya, 2009.
9. Rizvi, R. H., Dhyani, S. K., Newaj, R., Saxena, A. and Karmakar, P. S., Mapping extent of agroforestry area through remote sensing: issues, estimates and methodology. *Indian J. Agrofor.*, 2013, **15**(2), 26–30.
10. Ellis, E. A., Nair, P. K. R., Linehan, P. E., Beck, H. W. and Blanche, C. A., A GIS-based database management application for agroforestry planning and tree selection. *Comput. Electron. Agric.*, 2000, **27**, 41–55.
11. Bydekerke, L., Van Ranst, E., Vanmechelen, L. and Groenemans, R., Land suitability assessment for cherimoya in southern Ecuador using expert knowledge and GIS. *Agric. Ecosyst. Environ.*, 1998, **69**, 89–98.
12. Bernard, G. and Depommier, D., The systematic approach and the role of GIS in the characterization and monitoring of agroforestry parks. In XI World Forestry Congress, Antalya, Turkey, 13–22 October 1997, p. 87.
13. Paquette, S. and Domon, G., The transformation of the agroforestry landscape in the nineteenth century: a case study in Southern Quebec, Canada. *Landscape Urban Plan.*, 1997, **37**, 197–209.
14. Jasinski, M. F., Estimation of subpixel vegetation density of natural regions using satellite multispectral imagery. *IEEE Trans. Geosci. Remote Sens.*, 1996, **34**, 804–813.
15. Campbell, J. B., *Introduction to Remote Sensing*, The Guildford Press, New York, 2002, 3rd edn.
16. Dhyani, S. K., Newaj, R. and Sharma, A. P., Agroforestry: its relation with agronomy, challenges and opportunities. *Indian J. Agron.*, 2009, **54**, 249–266.
17. Walkley, A. J. and Black, C. A., Estimation of soil organic carbon by the chromic acid titration method. *Soil Sci.*, 1934, **37**, 29–38.
18. Schelhaas, M. J. *et al.*, CO2FIX V 3.1 – a modelling framework for quantifying carbon sequestration in forest ecosystems. ALTERRA Report 1068 Wageningen, The Netherlands, 2004.
19. Namburs, G. J. and Schelhaas, M. J., Carbon profile of typical forest types across Europe assessed with CO2FIX. *Ecol. Indic.*, 2002, **1**, 213–233.
20. Masera, O. *et al.*, Modelling carbon sequestration in afforestation, agroforestry and forest management projects: the CO2FIX V.2 approach. *Ecol. Model.*, 2003, **164**, 177–199.
21. Ajit, Dhyani, S. K. *et al.*, Modeling analysis of potential carbon sequestration under existing agroforestry systems in three districts of Indo-gangetic plains in India. *Agrofor. Syst.*, 2013, **87**(5), 1129–1146.
22. Rizvi, R. H., Newaj, R., Karmakar, P. S., Saxena, A. and Dhyani, S. K., Remote Sensing analysis of Agroforestry in Bathinda and Patiala districts of Punjab using sub-pixel method and medium resolution data. *J. Indian Soc. Remote Sensing*, 2015; doi: 10.1007/s12524-015-0463-3.
23. Kaul, M., Mohren, G. M. J. and Dadhwal, V. K., Carbon storage and sequestration potential of selected tree species in India. *Mitig. Adapt. Strateg. Glob. Change*, 2010, **15**, 489–510.
24. Palaniswami, C., Upadhyay, A. K. and Maheshwarappa, H. P., Spectral mixture analysis for sub-pixel classification of coconut. *Curr. Sci.*, 2006, **91**(12), 1706–1711.
25. Oki, K., Ojuma, H. and Sugita, M., Sub pixel classification of Aldar trees using multispectral Landsat Thematic Mapper Imagery. *Photogramm. Eng. Remote Sensing*, 2002, **68**(1), 77–82.
26. Rizvi, R. H., Dhyani, S. K., Yadav, R. S. and Singh, R., Biomass production and carbon stock of polar agroforestry systems in Yamunanagar and Saharanpur districts of north-western India. *Curr. Sci.*, 2011, **100**(5), 736–742.

ACKNOWLEDGEMENTS. This study was conducted under the National Initiative on Climate Resilient Agriculture Project. We thank the Indian Council of Agricultural Research (ICAR), New Delhi for financial and other support to this project.

Received 30 October 2015; revised accepted 20 January 2016

doi: 10.18520/cs/v110/i10/2005-2011

Green synthesis of copper bionanoparticles to control the bacterial leaf blight disease of rice

Antonymsamy Kala¹, Sebastin Soosairaj^{1,*},
Subramanian Mathiyazhagan² and
Prakasam Raja¹

¹Department of Botany, St Joseph's College (Autonomous),
Tiruchirappalli 620 002, India

²Krishi Vigyan Kendra, Vamban Colony, Pudukkottai 622 303, India

Copper bionanoparticles were successfully synthesized using leaf aqueous extract of *Datura innoxia* from copper sulphate. Nanoparticles were characterized with the help of UV–Vis spectroscopy, Field Emission Scanning Electron Microscopy (FESEM), Energy Dispersive X-ray Spectroscopy and Fourier Transform Infrared Spectroscopy. FESEM analysis showed that the particles were spherical in shape with size ranging

*For correspondence. (e-mail: pspsoosai@yahoo.co.in)

from 5 to 15 nm. The antimicrobial activity of copper bionanoparticles revealed that they are effective growth inhibitors against *Xanthomonas oryzae* pv. *oryzae*, the causative organism of bacterial leaf blight of paddy.

Keywords: Bacterial leaf blight, copper bionanoparticles, *Datura innoxia*, green synthesis, rice.

IN recent years, the biocidal properties of copper nanoparticles (CuNPs) are being widely used in treating wounds. They are used through processed bandages with low-cost preparation as well as exceptional physical and chemical properties^{1,2}. They have industrial usage such as gas sensors, catalytic processes, high-temperature superconductors, solar cells, and so on^{3,4}. Besides, their high surface-to-volume ratio makes them easily reactive to other particles, and increases their antimicrobial efficiency, thus enabling decrease in the microbial concentration by 99.9%. Green synthesis of CuNPs has been achieved by using microorganisms⁵ as well as higher plants⁶.

Datura innoxia (Solanaceae), the thorn apple native to America, was introduced in Africa, Asia, Australia and Europe⁷. It has whitish pubescent flowers and grows as weed in wastelands⁸.

Bacterial leaf blight caused by *Xanthomonas oryzae* pv. *oryzae* is one of the most severe diseases of rice⁹. It is also one of the oldest known diseases, first noted by farmers in Kyushu Province, Japan around 1884 (ref. 10). It is a vascular disease that produces tannish-grey to white lesions all along the veins in rice. The disease increases with plant growth, peaking in the flowering stage, while symptoms are noted as early as at the tillering stage¹¹.

For synthesizing copper bionanoparticles, both the precursor and the reducing agents were mixed in a clean beaker in 1 : 1 proportion¹². For reduction of Cu ions, 5 ml of filtered plant extract was mixed with 5 ml of freshly prepared 1 mM aqueous CuSO₄ solution and incubated for 1 h. The change in colour was noted from light yellow to sea green. The colour change indicates reduction into CuNPs.

The reduction of nanoparticles was monitored using the Perkin-Elmer, Lambda 35 double beam UV-visible spectrophotometer against distilled water used as a blank. The UV-visible spectrum was measured in the range 190–1100 nm. The morphology, size and elemental analysis of the prepared CuNPs were examined using Field Emission Scanning Electron Microscopy (FESEM) with EDAX (Carl Zeiss, SUPRA 55 model). Fourier Transform Infrared Spectroscopy (FTIR) spectra were obtained using a spectrophotometer (Spectrum RX 1, Perkin Elmer, Singapore) in the spectral region of 4000–400 cm⁻¹.

The biosynthesized CuNPs of aqueous extract of *D. innoxia* leaves can easily be monitored using UV-visible spectroscopy (Figure 1). Nano-sized particles exhibit

unique optical properties. There is an exponential decay Mie scattering profile with decreasing photon energy. In this study the absorption peaks of copper nanoparticles ranged from 236 to 262 nm, which has been confirmed by earlier published works¹³. Nanoparticle formation is strongly indicated by increase in the peak with increase in reaction time and concentration of biological extracts with salt ions. UV-Vis absorption spectrum shows peaks in surface plasmon resonance of nano-sized particles^{14,15}.

Typical FESEM image shows that the product mainly consists of particle-like copper nano-clusters with panoramic view; the size ranges from 90 to 200 nm and the shape of the particles is spherical. However, further observations using high magnification revealed that these

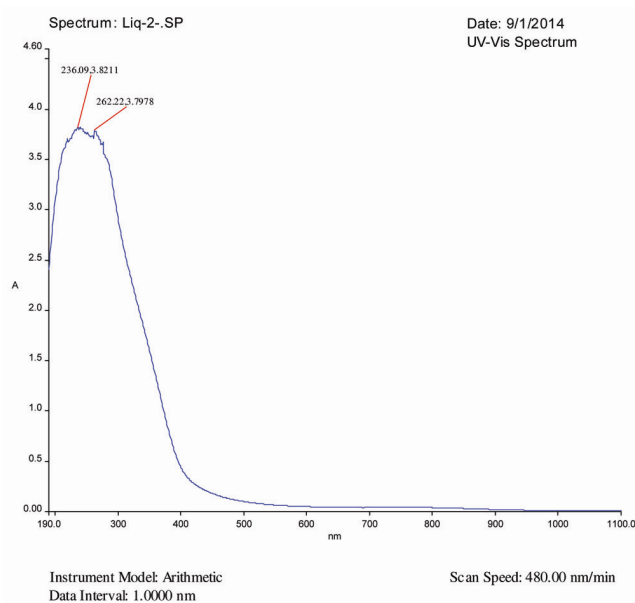


Figure 1. Ultraviolet-visible spectrum of bionanoparticles.

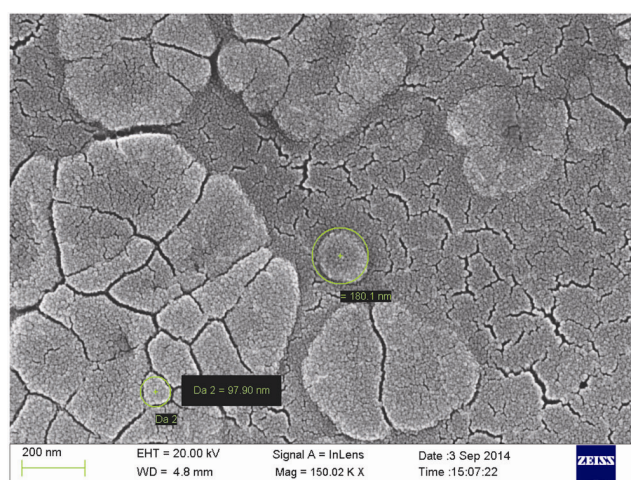


Figure 2. Field emission scanning electron microscopic image of bionanoparticles.

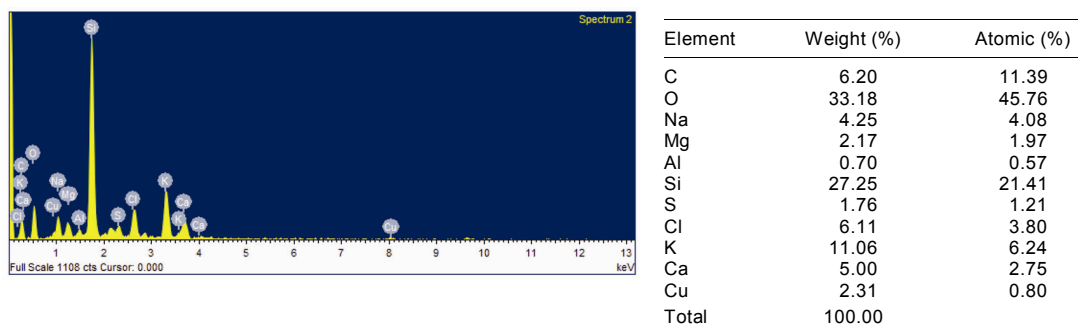


Figure 3. Energy-Dispersive X-ray Spectroscopic image of bionanoparticles.

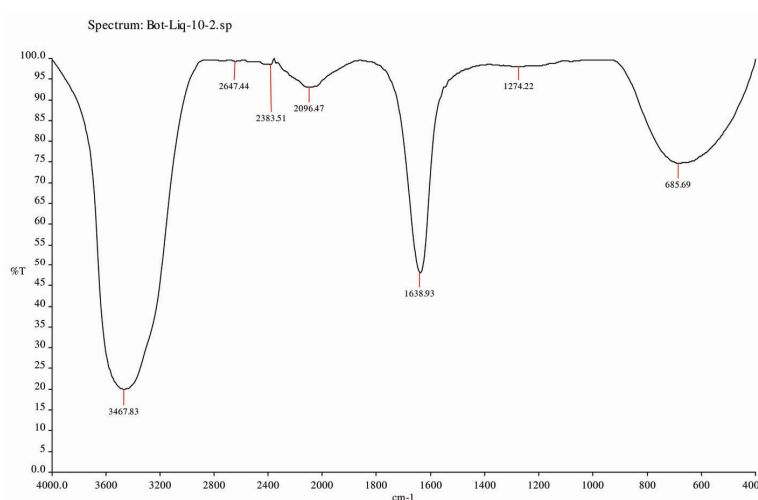


Figure 4. Fourier Transform Infrared Spectrum of bionanoparticles.

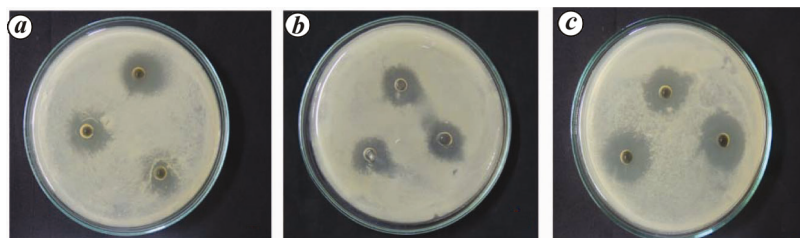


Figure 5. Antibacterial activity of *Datura innoxia* and its copper nanoparticles. *a*, *D. innoxia* leaf extract; *b*, Plantomycin chemical solution; *c*, Synthesized copper nanoparticles solution.

copper nano-clusters are assembled by smaller nanoparticles, which exhibit non-uniformity, and the average diameter is about 5–15 nm (Figure 2). The particle size was calculated using the software Image J (IJ). The Energy Dispersive X-ray Spectroscopy (EDX) analysis revealed that pure copper (2.31%) was present in the solution (Figure 3). The synthesized samples were transferred to the FESEM chamber for microstructural analysis without disturbing the actual nature of the products. The FESEM images confirm that the nanoparticles have grown with well-defined morphology¹⁶.

FTIR analysis was used to identify biomolecules that are responsible for capping and stabilization of CuNPs with *D. innoxia* leaf extract. A strong peak at 3434 cm^{-1}

can be attributed to hydrogen-bonded O–H groups of alcohols and phenols, and also to the presence of amines N–H of amide (Figure 4). This peak shifted to 3467 cm^{-1} in the synthesized CuNPs. The peak at 2256 cm^{-1} can be attributed N=C=O groups of isocyanates and Si–H silane stretch mode. The bands at 1638 cm^{-1} in *D. innoxia* leaf extract could be attributed to C–H stretch mode in aldehydes. The bands at 1461 and 1374 cm^{-1} are assigned to C–H deformation mode in alkanes. The bands at 1038 cm^{-1} are assigned to C–O stretch mode in ethers, while those at 687 cm^{-1} are assigned to C–Cl stretch mode in halogens. The bands at 2096 cm^{-1} can be attributed to diazo ketones and those 2383 cm^{-1} to P–H-phosphine in the synthesized CuNPs. The bands at

RESEARCH COMMUNICATIONS

Table 1. Growth inhibitory activity of *Datura innoxia* and its copper nanoparticles

Types of extract	Diameter of inhibition zone (mm)
Plant extract	17
Copper nanoparticles	24
Plantomycin	19

1274 cm^{-1} are assigned to C–H bend in plane bending bonds, and those at 685 cm^{-1} are assigned to C–H-strong vinyl mode in alkenes. This clearly indicates that the coordination of carboxylic acids in the protein of *D. innoxia* leaf extract with CuNPs plays a major role in dispersing, stabilizing and capping CuNPs. FTIR spectrum of CuNPs suggests that they are surrounded by different organic molecules such as alcohols, aldehydes and carboxylic acid¹⁷.

Antibacterial activity of the synthesized CuNPs was studied using well-diffusion method. The inhibitory effect of nanoparticles on bacterial growth was reflected by the zone of inhibition formed and comparison with known antibiotics (Table 1). Biosynthesized CuNPs showed clear zone of inhibition against *X. oryzae* pv. *oryzae*. Zone of inhibition was 24 mm for CuNP solution, 17 mm for *D. innoxia* leaf aqueous solution and 19 mm for plantomycin solution (antibiotic). Antibacterial activity of nanoparticles was assessed based on the zone of inhibition around the well (Figure 5). The results establish that the synthesized CuNPs have significant antibacterial action due to the greater affinity of copper ions to profusely present amines and carboxyl groups on the cell surface¹⁸. The extremely large surface area of CuNPs provides efficient antibacterial property by binding with the DNA molecules that leads to deformation of the helical structure by cross-linking of the nucleic acid strands¹⁹. Copper ions inside the bacterial cells also cause disruption of other biochemical processes²⁰.

The present work reports an eco-friendly, clean, non-toxic and simple process for synthesis of copper bio-nanoparticles using *D. innoxia* leaf aqueous extract. The synthesized CuNPs are highly stable and have been observed to possess antibacterial activity against rice pathogen *X. oryzae* pv. *oryzae* isolates from bacterial leaf blight diseased rice plant.

- Borkow, G. *et al.*, Molecular mechanisms of enhanced wound healing by copper oxide-impregnated dressings. *Wound Repair Regen.*, 2010, **18**(2), 266–275.
- Borkow, G., Zatzoff, R. C. and Gabbay, J., Reducing the risk of skin pathologies in diabetics by using copper impregnated socks. *Med. Hypotheses*, 2009, **73**(6), 883–886.
- Li, Y., Liang, J., Tao, Z. and Chen, J., CuO particles and plates: synthesis and gas-sensor application. *Mater. Res. Bull.*, 2008, **43**, 2380–2385.
- Guo, Z., Liang, X., Pereira, T., Scaffaro, R. and Hahn, H. T., CuO nanoparticle filled vinyl-ester resin nanocomposites: fabrication, characterization and property analysis. *Compos. Sci. Technol.*, 2007, **67**, 2036–2044.
- Honary, S., Barabadi, H., Gharaeifathabad, E. and Naghibi, F., Green synthesis of copper oxide nanoparticles using *Penicillium aurantigriseum*, *Penicillium citrinum* and *Penicillium waksmanii*. *Digest J. Nanomater. Biostruct.*, 2012, **7**, 999–1005.
- Gunalan, S., Sivaraj, R. and Venkatesh, R., *Aloe barbadensis* Miller. mediated green synthesis of mono-disperse copper oxide nanoparticles: optical properties. *Spectrochim. Acta Part A*, 2012, **97**, 1140–1144.
- Preissel, U. and Preissel, G. H., *Brugmansia and Datura: Angel's Trumpets and Thorn Apples*, Firefly Books, Buffalo, New York, 2002, pp. 106–123.
- Matthew, K. M., *The Flora of the Tamil Nadu Carnatic*, The Rapinat Herbarium, St Joseph's College, Tiruchirappalli, 1983, vol. 2, p. 718.
- Yoshimura, S. and Tahara, S. K., Morphology of bacterial leaf blight organism under (electron) microscope. *Ann. Phytopathol. Soc. Jpn.*, 1960, **26**, 61.
- Swings, J., Van den Mooter, M., Vauterin, L., Hoste, B., Gillis, M., Mew, T. W. and Kersters, K., Reclassification of the causal agents of bacterial blight (*Xanthomonas campestris* pv. *oryzae*) and bacterial leaf streak (*Xanthomonas campestris* pv. *oryzicola*) of rice as pathogens of *Xanthomonas oryzae* (ex. Ishiyama 1922) sp. nov., nom. rev. *Int. J. Syst. Evol. Microbiol.*, 1990, **40**, 309–311.
- Tagami, Y. and Mizukami, T., Historical review of the researches on bacterial leaf blight of rice caused by *Xanthomonas oryzae* (Uyeda et Ishiyam) Dowson [English translation by H. Fujii]. Ebook, Sustainable approaches to controlling plant pathogenic bacteria. In Report of Ministry of Agriculture Department of Japan (eds Kannan, V. R. and Bastas, K. K.), CRC Press, Taylor and Francis Group, NY, 1962, vol. 10, pp. 1–112.
- Subhankari, I. and Nayak, P. L., Synthesis of copper nanoparticles using *Syzygium aromaticum* (cloves) aqueous extract by using green chemistry. *World J. Nanosci. Technol.*, 2013, **2**(1), 14–17.
- Prema, P., Chemical mediated synthesis of silver nanoparticles and its potential antibacterial application. In *Progress in Molecular and Environmental Bio-engineering – From Analysis and Modelling to Technology Applications* (ed. Angelo Carpi), 2010, pp. 151–166; ISBN: 978-953-307-268-5.
- Abboud, Y., Saffaj, T., Chagraoui, A., El-Bouari, A., Brouzi, K., Tannane, O. and Hssane, B., Biosynthesis, characterization and antimicrobial activity of copper oxide nanoparticles (CONPs) produced using brown alga extract (*Bifurcaria bifurcate*). *Appl. Nanosci.*, 2014, **4**, 571–576.
- Swarnkar, R. K., Singh, S. C. and Gopal, R., Effect of aging on copper nanoparticles synthesized by pulsed laser ablation in water: structural and optical characterizations. *Bull. Mater. Sci.*, 2011, **34**(7), 1363–1369.
- Shah, M. and Al-Ghamdi, M., Preparation of copper (Cu) and copper oxide (Cu₂O) nanoparticles under supercritical conditions. *Mater. Sci. Appl.*, 2011, **2**(8), 977–980.
- Vasudev Kulkarni, B. and Pramod Kulkarni, S., Green syntheses of copper nanoparticles using *Ocimum sanctum* leaf extract. *Int. J. Chem. Stud.*, 2013, **1**(3), 1–4.
- Awad, A. M., Albiss, B. A. and Salem, N. M., Antibacterial activity of synthesized copper oxide nanoparticles using *Malva sylvestris* leaf extract. *SMU Med. J.*, 2015, **2**(1), 91–101.
- Beveridge, T. J. and Murray, R. G., Sites of metal deposition in the cell wall of *Bacillus subtilis*. *J. Bacteriol.*, 1980, **141**(2), 876–887.
- Kim, J. H., Cho, H., Ryu, S. E. and Choi, M. U., Effect of metal ions on the activity of protein tyrosine phosphatase VHR: highly potent and reversible oxidative inactivation by Cu₂C ion. *Arch. Biochem. Biophys.*, 2000, **382**(1), 72–80.

Received 11 August 2015; revised accepted 8 October 2015

doi: 10.18520/cs/v110/i10/2011-2014